ELSEVIER

Journal of Power Sources 56 (1995) 31–36

JOURNAL OF POWER SOURCES

Internal hydration H_2/O_2 100 cm^2 polymer electrolyte membrane fuel cell

Pile à combustible à membrane électrolyte polymère H_2/O_2 de 100 cm^2 à hydratation interne

S. Miachon, P. Aldebert

CEA/Département de Recherche Fondamentale sur la Matière Condensée, SESAM/PCM, 17 avenue des Martyrs, 38054 Grenoble Cedex 9, France

Received 28 December 1994; revised 16 February 1995; accepted 18 February 1995

Abstract

This work deals with a new arrangement of a polymer electrolyte membrane fuel cell (PEMFC) support which allows the operation of a 100 cm^2 surface area fuel cell with cold and unhumidified gases. Hydrogen is not recycled. Both gases (pure hydrogen and oxygen) are heated and humidified internally, each one crossing a porous carbon block. This allows a simplified water management. Classical low platinum loading E-Tek® electrodes, hot-pressed on Nafion® 117 and 112 membranes, are used. Performances are then a little higher than those of comparable PEMFCs in the literature: 0.7 V at 0.7 A/cm^2 for Nafion® 117, and 0.724 V at 1 A/cm^2 for Nafion® 112, under 4/6 bar (absolute) of H_2/O_2 at 100 °C. The values of PEMFC resistance obtained in fitting the data were found to be $R = 0.254$ (with Nafion® 117) and 0.108 Ω cm^2 (with Nafion® 112). The membrane contribution to the cell resistance was then estimated to be $R_m = 0.204$ and 0.058 Ω cm^2, respectively (with Nafion® conductivity estimated at 0.103 S/cm at 100 °C in working fuel cell conditions). This membrane is therefore the major contributor to the total cell resistance.

Résumé

Ce travail présente une nouvelle cellule de pile à combustible (PAC) à membrane électrolyte polymère (MEP). Notre système, de surface active de 100 cm^2, fonctionne sans recirculation d'hydrogène, avec des gaz froids et non hydratés au préalable. Les gaz (de l'hydrogène et de l'oxygène purs) sont en fait hydratés en interne, en traversant un fritté de carbone, ce qui permet une gestion de l'eau simplifiée. On utilise des électrodes E-Tek® à faible chargement de platine, imprégnées et pressées à chaud sur des membranes Nafion® 117 et 112. Les performances sont alors légèrement supérieures à celles de PAC MEP de la littérature: 0,7 V à 0,7 A/cm^2 pour le Nafion® 117, et 0,724 V à 1 A/cm^2 pour le Nafion® 112, sous 4/6 bar (absolus) de H_2/O_2 à 100 °C. Les valeurs de la résistance de pile R obtenues en ajustant les valeurs expérimentales, sont de 0,254 (avec le Nafion® 117) et 0,108 Ω cm^2 (avec le Nafion® 112). La fraction de cette résistance due à la membrane a été estimée à $R_m = 0{,}204$ et 0,058 Ω cm^2, respectivement (la conductivité du Nafion® étant alors estimée à 0,103 S/cm à 100 °C dans les conditions de fonctionnement de la pile). R_m est donc la composante majeure de la résistance de pile.

Keywords: Polymer electrolyte membrane fuel cells; Hydrogen; Oxygen

1. Introduction

Polymer electrolyte membrane fuel cells (PEMFCs) are an important research subject throughout the world [1–10]. As a matter of fact, the prospect of using them as non-polluting primary power sources for transportation, or lightweight sources in space, has initiated many R&D programmes all over the world.

A major factor in this field is water management. Membranes need an optimized water content in order to maintain a high protonic conductivity. Moreover, the amount of water in the whole electrode membrane assembly (EMA) has a major effect on the performances.

Classical PEMFC systems need complex external hydration devices that must be thermoregulated a few degrees °C higher than the cell [11–13]. External hydration places limitations on the stack design. Complementary elements

SSDI 0378-7753(95)02201-Q

for gas hydration must be added, and hydrogen has to be recycled. Some authors have designed low-performance fuel cells with internal hydration systems [14,15].

The purpose of this work is to optimize the fuel cell element, e.g., the hardware that brings the gases to and drives produced water out of the EMA. This is achieved by modifying the cell design through the introduction of a simplified water-management system within the element.

2. Limitations due to the support

2.1. Voltage–current profile

The power losses in a PEMFC depend on the current produced, according to the typical V–i curve illustrated in Fig. 1.

Part A is linked to the electrodes kinetics of catalysis (mainly at the cathode). Escribano [16] and Mosdale and Steven [17] and many other researchers elsewhere [8,18–22] are currently working on the improvement of the electrode performance.

The influence of hardware on this part is due to the water in the electrode. Nafion® used to make three-dimensional electrodes needs water to allow protons to access the platinum catalyst. Excess or lack of water limits the access of gas to the catalyst through the Nafion®-impregnated layer.

Proper cell water management should provide an appropriate amount in the electrode zone.

Part B shows losses mainly due to the ionic and electronic resistances of the element. In our case, it can be written as follows:

$$R = R_{im} + R_e + R_{ec} \quad (1)$$

where R_{im} is the ionic resistance of the membrane, R_e the ionic contact resistance between the membrane and the three-dimensional electrodes, and the electronic resistance of the electrodes, and R_{ec} the electronic contact and material resistance of the components in the cell between the electrode and the graphite block.

One can then add another contribution, if the cell potential is measured on copper current collector: R_{cc}, the electronic contact and material resistance between the graphite block and the external copper current collector.

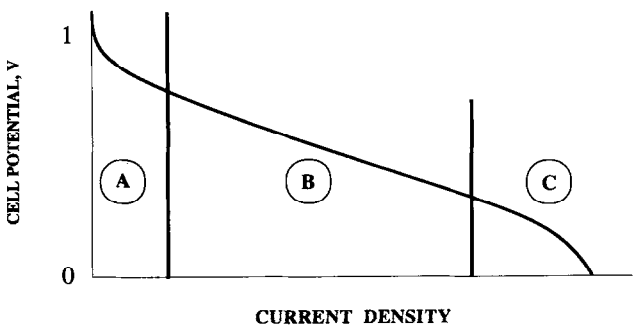

Fig. 1. Typical V–i profile showing the three zones: (A) activation; (B) ohmic loss, and (C) mass transport limitations.

To improve R, membranes with a lower resistance can be used (thinner Nafion® 112, 115, different ionomer Dow or Asahi experimental membranes, etc.), and one can try to establish a good ionic bond between the electrode and the membrane. Many authors have carried out experiments on PEMFCs with these new membranes and/or electrodes [23].

In this study, Nafion® 117 and 112 only are used in order to establish the influence of the membrane on the total PEMFC resistance. From the point of view of the support, we have to minimize contact and material resistances.

Part C deals with mass-transport limitation. Mosdale [24] and Srinivasan [25] have studied the influence of oxygen diffusion in the three-dimensional electrode on the performance of the cell. This diffusion depends on the amount of water in the electrode, and on the easy access of oxygen to the whole electrode. Hydrogen diffusion in the anode may also bring limitations.

The water and gas management in the support take then a great importance in avoiding flooding or drying out of the electrode, that allows satisfying the oxygen diffusion.

2.2. Dead zones

Further to this first rough analysis, we must bear in mind the need that the whole surface area of the EMA should be kept active, avoiding dead zones. A correct balance must be achieved between water content and gas access, in a homogeneous way.

3. Experimental

3.1. Electrode membrane assemblies

The EMAs used for this work were made using procedures described in Refs. [7,14,16] with Du Pont Nafion® 117 (0.175 mm thick) or 112 (0.05 mm) membrane and E-Tek ELAT electrodes and with 0.35 mg Pt/cm^2 on both sides of the anode and the cathode. These electrodes were impregnated with up to 1 mg of H^+ Nafion® per cm^2, before being pressed at 80 kN and 140 °C for about 90 s.

3.2. Hardware

The classical PEMFCs use machined graphite blocks with rib-channel patterned gas feeders on the side in contact with electrodes. The working principle of our cell is slightly different. Instead of flowing along channels, the gases have to pass through a porous carbon block in order to reach the electrode, as shown in Fig. 2.

This arrangement enables us:

- to keep liquid water in the oxygen chamber at high temperatures (up to 120 °C under 6 bar absolute pressure, depending on the oxygen flow)
- to bring water produced at the cathode to the hydrogen chamber

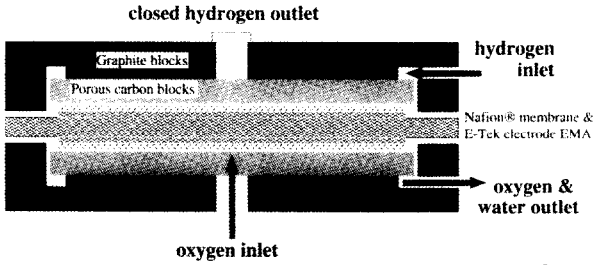

Fig. 2. Schematic drawing of the gas feeding principle in the 100 cm^2 internal hydration PEMFC.

- to avoid uneven mechanical compression on the EMA (no channels)
- to work with different oxygen flows without any critical consequences

The pressure drop between the oxygen inlet and outlet has been measured at less than 0.01 bar. The porous carbon blocks have been selected for their hydrophilicity.

3.3. Experimental conditions

The EMA is inserted dry in the PEM support. Half an hour at 0.2 V allows sufficient membrane hydration so that 1 A/cm^2 can be achieved. It is then maintained at 1 A/cm^2 for 24 h.

Pure hydrogen and oxygen were used under 4 and 6 bar (absolute) pressure, respectively. The pressure drop between the cathode and anode chambers was maintained in order to help the back diffusion of water produced at the cathode into the anode porous carbon block.

Tests were done at 80 and 100 °C. The temperature is processor-controlled by a thermostated oil circuit in the support.

The oxygen flow was computer-controlled through a microprocessor-controlled pneumatic valve. It was kept proportional to the current, the excess gas being used for the water exhaust.

The hydrogen flow was maintained at the stoichiometric requirements of the cell, while the outlet was closed. The electronic loading device (made by SONEA, Apprieu, 38, France) allowed a current from 0 to 100 A (that is to day 0 to 1 A/cm^2) over the whole potential range (0–1.1 V).

Water produced in the cell was stored in a scaled reservoir in order to check that no excess water was accumulated in the cathode chamber.

The cell compression force was 27 kN.

3.4. Measurements

Data on temperature, pressure, gas-flow rates, current and potential were stored by computer controlling. The sampling time for all measurements was only a few seconds. The potential was measured at six positions in order to evaluate the different components of the cell resistance, as shown in Fig. 3. Three voltage drops were obtained and measured through a filtered amplifier (SONEA) in order to eliminate noise.

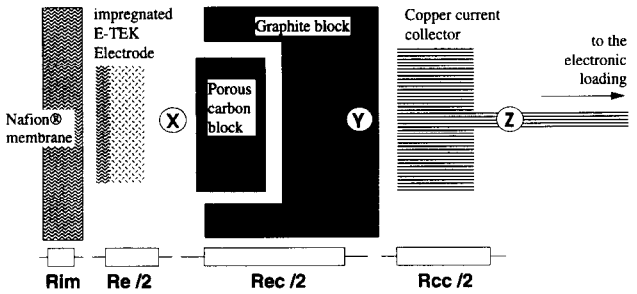

Fig. 3. Schematic drawing (half-cell) of the cell resistance components (X, Y, Z refer to potential measurement points).

This allowed a precision of 0.25 mV on a National Instrument acquisition card in a Macintosh IISi microcomputer. Potentials at Z and Y were measured using pointed probes. Two 0.1 mm polytetrafluoroethylene-coated gold wires were inserted on each side of the EMA, at X, in order to measure the potential at the electrode. The 'cell potential' shown in the following results was measured on graphite blocks (at Y), described earlier in Ref. [25].

3.5. Stability

The cell was maintained at a computer-controlled current density (via the SONEA load) as long as the graphite potential (measured at Y, see Fig. 3) was stabilized, and kept at this value for about 10 min. It generally took less than 1 min to reach this steady-state working point.

In any case, a value of the current density established at 0.7 V (i.e., 0.7 A/cm^2 for Nafion® 117 and 1 A/cm^2 for Nafion® 112, respectively) has been maintained over a longer period of time (100 and 25 h, respectively). We can be reasonably sure that the values for the V–i profiles presented here are stable.

4. Results

4.1. Voltage–current profiles

The performances measured on Nafion® 117 EMAs at 80 and 100 °C were similar (0.6 and 0.7 A/cm^2 at 0.7 V). We could only detect the onset of mass-transport limitations at 80 °C above 0.7 A/cm^2, see Fig. 4. Nafion® 112 exhibited better results, as this membrane is 3.5 times thinner. Moreover, it seemed that there are no mass-transport limitations at the current densities used (Fig. 5).

Parts A and B (excluding the mass-transport limitation zone) of fuel cell with the V–i profiles can be least-squared fitted by Eq. (2) [26,27]:

$$V = E_0 - b \log(i) - Ri \quad (2)$$

with

$$E_0 = E_{th} + b \log(i_0) \quad (3)$$

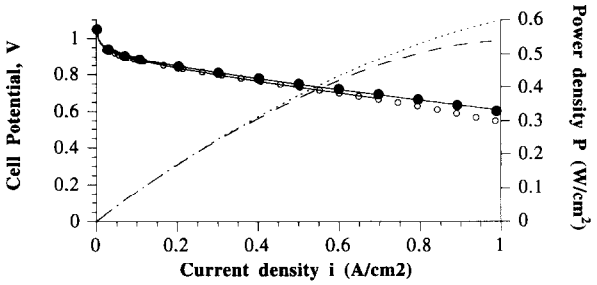

Fig. 4. Fuel cell potential–current density profiles (with power density) for Nafion® 117 EMAs with E-TEK ELAT electrodes loaded at 0.35 mg Pt/cm² under 4/6 bar pressure of H_2/O_2: (○) potential at 80 °C; (●) potential at 100 °C); (– –) power density at 80 °C, and (...) power density at 100 °C, lines on the potential points plot Eq. (2) fits.

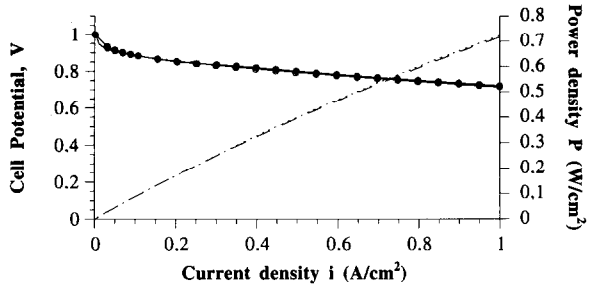

Fig. 5. Fuel cell potential–current density profiles (with power density) for Nafion® 112 EMAs with E-TEK ELAT electrodes loaded at 0.35 mg Pt/cm² under 4/6 bar pressure of H_2/O_2: (○) potential at 80 °C; (●) potential at 100 °C; (– –) power density at 80 °C, and (...) power density at 100 °C, lines on the potential points plot Eq. 2 fits.

Table 1
Values of the fitting parameters for the cell *V–i* profiles for Nafion® 117 and 112 membranes EMAs with Nafion® impregnated 0.35 mg Pt/cm² E-Tek® electrodes, tested at 80 and 100 °C, under 4/6 bar pressure

Nafion®	Temperature (°C)	Fitting field (A/cm²)	R (Ω cm²)
117	80	0.01–0.7	0.281 ± 0.005
117	100	0.01–1	0.254 ± 0.005
112	80	0.01–1	0.114 ± 0.001
112	100	0.01 ± 1	0.108 ± 0.005

where the parameters b (Tafel slope) and i_0 (exchange-current density) are a function of the properties of the cathode catalytic layer. They control part A in Fig. 1. E_{th} is the thermodynamic reversible potential for the fuel cell reaction. In our pressure and temperature conditions, this parameter has been evaluated by Mosdale [28]. Under 4/6 bar absolute pressure, E_{th} is 1.20 and 1.18 V at 80 and 100 °C, respectively. The values measured previously were comparable with those published for these electrodes ($b = 0.07$ V/dec and $i_0 \approx 10^{-3}$ mA/cm² of electrode geometric area [29]). The purpose of this study was to evaluate the different resistive components in a PEMFC element. Using Eq. (2), the experimental data are given in Table 1.

4.2. Cell resistance and Nafion® conductivity

The potential was measured at different points in the fuel cell fixture, Fig. 3. This study revealed that all the components of the resistance increased slightly with the current density (a few percent over the 0–1 A/cm² range). This has not been verified in the case of R_m, the ionic membrane resistance, for which we only have the Eq. (2) fit estimates.

The values for the different resistive components, were determined as follows:

(i) R_{ec} was measured by the voltage drop between the graphite blocks and the gold wire directly in contact with the E-Tek® electrode;

(ii) R_e and R_m were determined using the following equations (R' and R'' are the values of R in the Eq. (2) fits respective to Nafion® 117 and 112 membrane EMAs, determined earlier):

$$R_{m117} + R_e + R_{ec} = R' \quad (4)$$

$$R_{m112} + R_e + R_{ec} = R'' \quad (5)$$

considering that the membrane resistance is proportional to the thickness, $R_{m117} = 3.5\, R_{m112}$, and $(R_e + R_{ec})$ is membrane independent.

The values found for the membrane resistance were in good agreement with the conductivity of Nafion®, as measured by Yeo [30], for example, $\sigma = 0.112$ S/cm, for the optimum water content $(20H_2O)/SO_3^-$ at 80 °C. The thicknesses of the swelled Nafion® 112 and 117 membranes were measured as $l_{112} = 0.06$ mm and $l_{117} = 0.21$ mm. Therefore, $R_{m112} = 0.053$ Ω cm² and $R_{m117} = 0.188$ Ω cm², Table 2. The small difference between the measured and computed membrane resistance is probably due to a non-homogeneous water content of the Nafion® membrane.

We can present the following values for Nafion® conductivity in another way, indirectly measured by our apparatus, in the working fuel cell conditions:

- $\sigma = 0.091$ S/cm at 80 °C
- $\sigma = 0.103$ S/cm at 100 °C

R_{cc} is measured between Y and Z (see Fig. 3). It indicates the ohmic loss in the end-plate of a stack using this technology. Nevertheless, it has not been optimized further than adding some grease between the graphite block and the copper current collector (Fig. 3).

4.3. Energetic yield rate

The energetic yield rate has been defined by Gaggioli et al. [31] as the total provided Gibbs energy/collected electrical Gibbs energy.

The whole fuel cell process occurs in isothermal conditions at the cell temperature T_c, and the only reaction product is liquid water coming out of the electrode. This total yield rate can then be computed considering the following reaction:

$$H_2^{g,T_c} + \tfrac{1}{2} O_2^{g,T_c} \longrightarrow H_2O^{l,T_c} \quad (6)$$

The Gibbs reaction is [32]:
$\Delta G = 225.6$ kJ/mol at 100 °C, and $\Delta G = 228.8$ kJ/mol at 80 °C.
The yield rate is:

Table 2
Values of the cell resistance components. R is the total resistance of the cell measured at Y, comprising: R_m (ionic membrane resistance); R_e (electrode resistance); R_{ec} (resistance between the electrode and the graphite block), but not comprising R_{cc} (contact resistance between the graphite block and the copper current collector)

Temperature (°C)	R (Ω cm^2)				R_{cc} (Ω cm^2) (not a part of R)
	R_m		R_e	R_{ec}	
	Nafion® 117	Nafion® 112			
100 experimentally	0.204	0.058	0.022	0.028	0.023
80 experimentally	0.233	0.067	0.020	0.029	0.025
80 (from Ref. [30])	0.188	0.053			

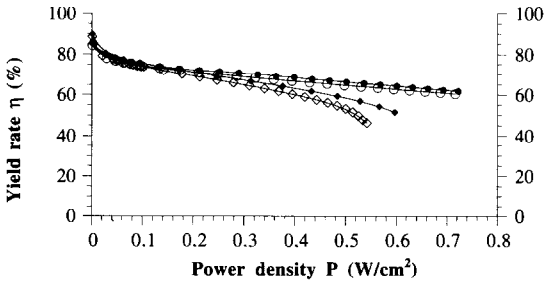

Fig. 6. Plot of the cell total yield rate for different EMAs at two temperatures: (♦) Nafion® 117 at 100 °C; (○) Nafion® 112 at 80 °C, and (●) Nafion® 112 at 100 °C.

$$\eta = \frac{nFU}{\Delta G} \tag{7}$$

where V is the cell potential, $F = 96\,487$ C/mol, and $n = 2$ electrons.

The total electric yield rate is plotted as a function of power density in Fig. 6.

The ideal working regime for the fuel cell is to achieve the highest power density at the highest possible yield rate. This rate was found to be 0.5–0.6 W/cm^2 (i.e., at a potential about 0.6–0.7 V) for Nafion® 117 membrane EMAs at 80 and 100 °C and avoids the fall in the yield rate at higher power densities.

For Nafion® 112 membrane EMAs, this ideal working regime occurs at a higher power density (and at a potential lower than 0.7 V). At the current densities tested, a fall in the yield rate was not observed.

5. Conclusions

The feasibility of running a PEMFC with unhumidified gases has been demonstrated for Nafion® 112 and 117 membranes. The Nafion® 112 membrane offered a much higher power density when correctly hydrated, because of its lower resistance, than the Nafion® 117 membrane.

The performances of the PEMFC, demonstrated in this work, were a little higher than those reported in the literature with traditionally prepared E-Tek electrodes [27,29,33]. A small test fixture resistance allowed higher power density. In fact, the biggest part of the element resistance was the EMA itself: even with Nafion® 112, the sum $R_m + R_e$ (EMA total resistance) was responsible for more than 77% of the ohmic losses. This value reached 88% with Nafion® 117. No further reduction in the cell element resistance would bring significant improvement in the performances. But new optimized EMAs would dramatically enhance the performance. A good indication of the yield rate behaviour was obtained. Nevertheless, to determine the ideal working regime for Nafion® 112 membrane EMAs, the current density must be increased. This will soon be achieved with a new 300 A load unit.

Acknowledgements

This work has been supported by ADEME and the VPE-PAC French Fuel Cell Program. The Nafion® 112 membrane sample has been supplied by Walther Grot, Du Pont Polymers. The authors also thank R. Vacher for his technical assistance.

References

[1] W.A. Adams and J.H. Morgan, *Electr. Vehicle Development, 8* (1989) 5–9.
[2] L.E. Alexander and G.A. Eisman, *World Patent No. WO 86/06879* (1986).
[3] R. Baldwin, M. Pham, A. Leonida, J. McElroy and T. Nalette, *J. Power Sources, 29* (1990) 388–412.
[4] D.M. Bernardi and M.W. Verbrugge, *J. Electrochem. Soc., 139* (1992) 2477–2491.
[5] R.E. Billings, M. Sanchez, P. Cherry and D.B. Eyre, *Int. J. Hydrogen Energy, 16* (1991) 829–837.
[6] J.Y. Catrin, *CEA Technol., 14* (May–June) (1994) 4.
[7] H.P. Dhar, *J. Electroanal. Chem., 357* (1993) 237–250.
[8] D.G. Epp and B.I. Wiens, *US Patent No. 5 176 966* (1993).
[9] W. Gramatte and G. Sandstede, *ETZ, 114* (1993) 280–285.
[10] C. Lamy and J.-M. Léger, *J. Phys. (Paris), 4* (1994) C1-253–281.
[11] S. Srinivasan and S. Somasundaram, in R.E. White and A.J. Appleby (eds.), *Proc. Symp. Fuel Cells, San Francisco, CA, USA, 6–7 Nov. 1989*, The Electrochemical Society, Pennington, NJ, USA, p. 71.
[12] S. Srinivasan, O. Velev, A. Parthasarathy and D. Manko, *J. Power Sources, 36* (1991) 299–320.

[13] D.S. Watkins, K.W. Dircks and D.G. Epp, *US Patent No. 5 108 849* (1992).
[14] P.M. Schütz, in R.E. White and A.J. Appleby (eds.), *Proc. Symp. Fuel Cells, San Francisco, CA, USA, 6–7 Nov. 1989,* The Electrochemical Society, Pennington, NJ, USA, p. 87.
[15] M. Watanabe, Y. Satoh and C. Shimura, *J. Electrochem. Soc., 140* (1993) 3190–3193.
[16] S. Escribano, *Thesis,* DEA d'Électrochimie de l'INP, Grenoble, France, Sept. 1992, p. 3.
[17] R. Mosdale and P. Stevens, *Solid State Ionics, 61* (1993) 251–255.
[18] J. Manassen and I. Cabasso, *Proc. 34th Int. Power Sources Symp., Cherry Hill, NJ, USA, 25–28 June 1990,* Institute of Electric and Electronic Engineers, New York, NY, USA, pp. 408–410.
[19] J.M. McIntyre, J.D. Birdwell, W.P. Carl and B.R. Smith, *Eur. Patent Applic. No. 0 228 602 A1* (1986).
[20] R. Mosdale, M. Wakizoe and S. Srinivasan, *Proc. San Francisco Electro-Chemical Society Meet., 1994,* in press.
[21] P.D. Naylor, R.T. Barton, P.J. Mitchell, J.B. Lakeman and K.E. Jordan, in T. Keily and B.W. Baxter (eds.), *17th Int. Power Sources Symp., Bournemouth, UK, 8–11 Apr. 1991,* Internal Power Sources Symp. Committee, Leatherhead, UK, p. 253.
[22] M.S. Wilson and S. Gottesfeld, *J. Applied Electrochem., 22* (1992) 1–7.
[23] Y.W. Rho, O.A. Velev, S. Srinivasan and Y.T. Kho, *J. Electrochem. Soc., 141* (1994) 2084–2096.
[24] R. Mosdale and S. Srinivasan, *Electrochim. Acta, 40* (1995) 413–421.
[25] S. Srinivasan, personal communication.
[26] S. Srinivasan, E.A. Ticianelli, C.R. Derouin and A. Redondo, *J. Power Sources, 22* (1988) 359.
[27] S. Srinivasan, D.J. Manko, H. Koch, M.A. Enayetullah and A.J. Appleby, *J. Power Sources, 29* (1990) 367–387.
[28] R. Mosdale, *Ph.D. Thesis,* INP, Grenoble, France, 1992, p. 41.
[29] S. Besse, Y. Naimi and A. Tounsi, personal communication (June 1994).
[30] R.S. Yeo, *J. Electrochem. Soc., Electrochem. Sci. Technol., 130* (1983) 533.
[31] R.A. Gaggioli and W.R. Dunbar, *J. Energy Sources Technol., 115* (1993) 100–104.
[32] O. Kubaschewski, C.B. Alcock and P.J. Stencer, *Materials Thermochemistry,* Pergamon, Oxford, 6th edn., 1993.
[33] T.E. Springer, T.A. Zawodzinski and S. Gottesfeld, *J. Electrochem. Soc., 138* (1991) 2334–2342.